HHS Public Access

Author manuscript

Mol Pharm. Author manuscript; available in PMC 2021 October 29.

Published in final edited form as:

Mol Pharm. 2019 December 02; 16(12): 4878–4889. doi:10.1021/acs.molpharmaceut.9b00763.

In Vivo Brain Delivery and Brain Deposition of Proteins with Various Sizes

Kavisha R. Ulapane[1], **Brian M. Kopec**[1], **Teruna J. Siahaan**[*]

Department of Pharmaceutical Chemistry, The University of Kansas, 2095 Constant Avenue, Lawrence, Kansas 66047, USA

Abstract

It is very challenging to develop protein drugs for the treatment of brain diseases; this is due to the difficulty in delivering them into the brain because of the blood-brain barrier (BBB). Thus, alternative delivery methods need further exploration for brain delivery of proteins to diagnose and treat brain diseases. Previously, ADTC5 and HAV6 peptides have been shown to enhance the *in vivo* brain delivery of small- and medium-size molecules across the BBB. This study was carried out to evaluate ability of ADTC5 and HAV6 peptides to enhance delivery of proteins of various sizes, such as 15 kDa lysozyme, 65 kDa albumin, 150 kDa IgG mAb, and 220 kDa fibronectin, into the brains of C57BL/6 mice. Each protein was labeled with IRdye800CW, and a quantitative method using near IR fluorescence (NIRF) imaging was developed to determine the amount of protein delivered into the brain. ADTC5 peptide significantly enhanced brain delivery of lysozyme, albumin, and IgG mAb but not fibronectin compared to controls. In contrast, HAV6 peptide significantly enhanced the brain delivery of lysozyme but not albumin and IgG mAb. Thus, there is a cut-off size of proteins that can be delivered by each peptide. The distribution of delivered protein in other organs such as liver, spleen, lung, kidney, and heart could be influenced by HAV6 and ADTC5. In summary, ADTC5 is a better BBB modulator than HAV6 in delivering various sizes of proteins into the brain, and the size of the protein affects its brain delivery.

Graphical Abstract

[*]Corresponding Author: Dr. Teruna J. Siahaan, Department of Pharmaceutical Chemistry, The University of Kansas, 2095 Constant Avenue, Lawrence, Kansas 66047, USA, siahaan@ku.edu, Phone: 785-864-7327, Fax: 785-864-5736.

[1]Both authors contributed equally to this work

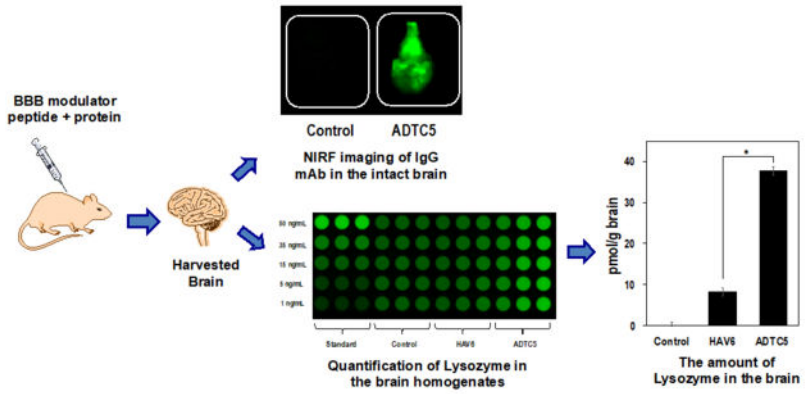

Keywords

blood-brain barrier; cadherin peptides; protein brain delivery; paracellular pathway; in vivo brain delivery

INTRODUCTION

Currently, protein drugs are a successful class of therapeutics for treating a wide variety of diseases such as cancers, infectious agents, genetic disorders, and autoimmune diseases (*e.g.,* type-1 diabetes (T1D), rheumatoid arthritis (RA), and multiple sclerosis (MS)). Protein therapeutics are normally developed with a specific and known mechanism of action and have reduced toxicity compared to small molecule drugs.[1] Some proteins such as brain-derived neurotrophic factor (BDNF),[2] nerve growth factor (NGF),[3] and insulin-like growth factor 1 (IGF-1)[4] have been investigated for inducing neuroregeneration in brain diseases such as MS and Alzheimer's (AD). Unfortunately, previous attempts to deliver proteins via the systemic circulation have met with only limited success due to the presence of the blood-brain barrier (BBB), which prevents them from entering the brain.[5–7] Monoclonal antibodies (mAbs), the fastest growing type of drugs, have also been investigated to treat brain diseases.[8] Several mAbs such as anti-Nogo-A,[9] anti-LINGO-1,[10] sHIgM22,[11] and VX15/2503[12] have been evaluated in clinical trials for inducing remyelination in MS patients; however, the clinical trials for most of these molecules were terminated due to their lack of efficacy in MS patients. A similar fate befell amyloid beta (Aβ) mAbs, which failed to effectively treat AD patients. Although many reasons could contribute to these failures, one potential problem is their inability to cross the BBB effectively from the blood into the brain.

The BBB is a selective barrier between the blood stream and the brain that prevents unwanted molecules from entering the brain. Many drug molecules cannot readily cross the BBB because the molecules need to have appropriate physicochemical properties for crossing the BBB. Most molecules that can passively cross the BBB can be predicted using the Lipinski's rule of five.[13] Because proteins do not satisfy this rule, BBB passive diffusion of proteins is very limited unless the protein has its own transporter on the endothelial microvessels for its transcytosis across into the brain. Therefore, there is a need

to develop methods to improve protein delivery into the brain in a non-invasive manner. Currently, many invasive ways such as intracerebral ventricular (ICV) delivery have been used to directly administer protein drugs into the brain in critical brain diseases. One of the limitations of the direct delivery method is the potential increase in brain infection and inflammation due to exposure to the outside environment. Currently, many non-invasive methods are being developed for enhancing brain drug delivery utilizing prodrug technology, receptor-mediated transcytosis mechanisms,[7] microbubble enhanced diagnostic ultrasound (MEUS) system,[14] intranasal delivery,[15] and BBB modulation.[16, 17] A BBB modulation method called “osmotic BBB delivery” has been successfully used to deliver antitumor drugs for treating brain tumor patients.[18] The osmotic BBB delivery method utilizes a hypertonic mannitol solution to disrupt the intercellular junctions of the BBB by shrinking the microvessel endothelial cells to allow anticancer drugs to passively penetrate the paracellular pathway of the BBB. Thus, the clinical success of the osmotic method provides impetus to investigate other ways to modulate the intercellular junctions of the BBB to improve brain delivery.

One way to modulate the BBB intercellular junctions in a controlled and selective way is by inhibiting cadherin-cadherin interactions that mediate cell-cell adhesion. Thus, we designed cadherin peptides such as HAV6 and ADTC5 to inhibit cadherin-cadherin interactions in a dynamic and equilibrium fashion to increase the porosity of the paracellular pathways reversibly and allow molecules to cross the BBB from the blood stream into the brain. HAV6 peptide can enhance the *in vivo* brain delivery of small molecules (*e.g.*, ^{14}C-mannitol, ^{3}H daunomycin, and gadopentetic acid (Gd-DTPA), IRdye R800, adenanthin), and large molecules (*e.g.*, 25 kDa IRdye800CW-polyethylene glycol and 65 kDa galbumin).[19–24] Similarly, ADTC5 peptide enhances brain delivery of ^{14}C-mannitol, Gd-DTPA, 8–12 amino acid peptides, and galbumin.[17, 22] Recently, HAV6 has been shown to effectively deliver adenathin, an anticancer agent, into the brain to suppress medulloblastoma brain tumor in mice.[24] In addition, HAV6 also significantly enhanced oral and brain delivery of eflornithine, an efflux pump substrate, in rats.[25] These data support the idea that modulation of cadherin-mediated cell-cell adhesion in the intercellular junction can improve drug delivery across the biological barriers (i.e., intestinal mucosa barrier and BBB).

In this study, the modulatory activities of HAV6 and ADTC5 were compared for brain delivery of different sizes of proteins such as 15 kDa lysozyme, 65 kDa albumin, 150 kDa IgG mAb, and 220 kDa fibronectin. To accomplish this, the proteins were conjugated with IRdye800CW on lysine residues and the protein brain depositions were determined quantitatively using NIRF imaging. The quantification method was developed and validated using standard curves of homogenized brain containing the IRdye800CW-conjugate protein. The method of validation to generate quantitative data for delivered protein was carried out by determining the stability, accuracy, precision, and linear dynamic range of the quantitation method. This study provides the difference between the effectiveness of HAV6 and ADTC5 for delivering different sizes of proteins as well as the size limit of the protein that each peptide can deliver through the BBB. The effects of each peptide on depositions of each protein in different organs, including liver, kidney, heart, spleen and lungs, were also determined.

MATERIALS AND METHODS

Chemicals, Reagents, and Animals.

Gyros Protein Technologies, Inc. (Tucson, AZ) was used as a vendor to purchase amino acids and coupling reagents for the automated peptide synthesizer. IRdye-800CW-NHS ester and IRdye-800CW Donkey anti-Goat IgG were purchased from LI-COR, Inc. (Lincoln, NE). Sigma Aldrich Chemical Company (St. Louis, MO) and Fisher Scientific, Inc. (Hampton, NH) were used as suppliers or proteins and reagents in this study. Protocols used for all animal studies have been approved by the Institutional Animal Care and Use Committee (IACUC) at The University of Kansas. All animals were cared by the Animal Care Unit personnel at The University of Kansas under the supervision of Veterinarians.

Peptide Synthesis and Purification.

The synthesis of the linear or cyclic peptides (Table 1) was accomplished using a Tribute solid-phase peptide synthesizer from Gyros Protein Technologies, Inc. (Tucson, AZ). A TFA solution containing scavengers was used to cleavage the peptide from the resin followed by addition of the TFA solution into cold diethyl ether to precipitate the peptide. To form cyclic ADTC5 peptide with a disulfide bond, the linear precursor was dissolved in high dilution using bicarbonate buffer solution at pH 9.0 followed by bubbling air into the peptide solution. The resulting oxidation reaction contained a high yield of the desired cyclic monomer with minimal amounts of side products (e.g., dimers and oligomers). The monomer was isolated from the mixture using a semi-preparative C18 column Waters XBridge C18 (19 mm × 250 mm, 5 μm particle size; Waters Corporation, Milford, MA)) in HPLC. The purity of each isolated fraction was determined by analytical HPLC using C18 column (Luna C18 (4.6 mm × 250 mm, 5 μm particle size, 100 Å; Phenomenex, Inc., Torrance, CA)). The identity of each peptide was confirmed by mass spectrometry.

Conjugation of Proteins with IRdye-800CW-NHS Ester.

Lysozyme, albumin, and fibronectin used in this study were conjugated with IRdye-800CW according to the manufacturer's instructions. Briefly, dyes were reacted with 1 mg/mL of protein in PBS with 10% potassium phosphate buffer, pH 9 (v/v) for 2 h at 25 °C. The resulting conjugates were purified using a spin column called Zeba Spin Desalting Column with 7 kDa molecular weight cut-off (Fisher Scientific, Inc. (Hampton, NH)). The purity of each conjugate was determined using SDS-PAGE, and the conjugate band was scanned (Excitation = 778 nm; Emission = 794 nm) with an Odyssey CLx NIR scanner to ensure that there was no free IRdye-800CW in the protein conjugate solution. Once any free dye was removed, the degree of labeling was determined using a UV spectrophotometer (Varian Cary 100, Agilent) to measure the fluorophore absorption and the protein absorbance at 280 nm, corrected for the fluorophore.

The protein concentration is calculated using the formula,

$$Protein\ Conc.\ \left(\frac{mg}{mL}\right) = \frac{A_{280} - (0.03 \times A_{780})}{\varepsilon_{Protein}} \times MW_{Protein} \times Dilution\ Factor$$

in which 0.03 was utilized as a correction factor for IRDye-800CW absorbance; the absorbance at 280 nm equals to 3.0% of the absorbance at 780 nm. $\varepsilon_{Protein}$ was designated as the molar extinction coefficient of the protein and molecular weight of the protein was designated as $MW_{Protein}$.

NIRF Method to Quantify Protein Amount in the Brain.

Preparation of Stock and Standard Curves.—The stock solution for IRDye800CW protein (*i.e.,* lysozyme, 70 μg/mL) was prepared and stored at –80 °C. The stock solution was later diluted with PBS to make the required standard solutions. To produce a standard calibration curve, 200 μL of blank brain homogenates was spiked with 10 μL standard solutions of various concentrations to yield a linear range from 0.5 to 50 ng/mL. The same method was employed for the sample's quality control (QC).

Accuracy and Precision.

For precision studies, IRDye-800CW-lysozyme was used. Brain homogenates were spiked with protein at concentrations between 0.5 and 50 ng/mL for determining the intra-day and inter-day, accuracy and precision.

Evaluation of Method Stability.

To evaluate stability of the quantitative method, IRDye-800CW-labeled lysozyme was used in spiked brain homogenates under various temperature and storage conditions. Three sets of samples were prepared to evaluate these various conditions. First, the samples were incubated at room temperature for 6 h before analysis. Second, the samples were incubated at −20 °C for 24 h with subsequent unassisted thawing at room temperature. Third, the samples were subjected to three freeze-thaw cycles between −20 °C and room temperature over a 24-h period prior to analysis. These stability studies were accomplished using protein concentrations from 0.5 to 50 ng/mL and three repeats for each sample group.

Brain Delivery IRdye800CW-labeled IgG mAb using ADTC5 in SJL/elite Mice.

For initial evaluation of whether a cadherin peptide can deliver proteins into the brain, IRdye800CW donkey-anti-goat IgG mAb was administered via i.v. with and without ADTC5 peptide in 5–8-week-old SJL/elite mice. Two groups of healthy SJL/elite mice were injected with (a) a mixture of IgG mAb (26.8 nmol/kg) and ADTC5 peptide (13 μmol/kg) (n = 5) and (b) IgG mAb alone (26.8 nmol/kg) (n = 4). After 15 min in the systemic circulation, the mice were euthanized using CO_2 inhalation followed by brain perfusion using PBS to remove the remaining protein in the BBB microvasculature. Next, the brains were isolated followed by NIRF imaging using Licor Odyssey CLx (Licor, Lincoln, NE). Eight optical sections were taken at 0.5 mm increments beginning from the bottom surface of the brain to a depth of 4 mm. The optical sections were summed to yield a fluorescence intensity value per each brain.

Comparison of HAV6 and ADTC5 in Delivering Various Sizes of Proteins into C57BL/6 Mice.

The BBB modulatory activities of ADTC5 and HAV6 to enhance brain delivery of IRdyeR800CW-labeled lysozyme, albumin, IgG mAb, and fibronectin were compared in C57BL/6 mice with 3 animals per group. The proteins with or without 13 μmol/kg HAV6 or ADTC5 were administered via tail vein injection. For lysozyme, the delivered doses were 21.6 and 54 nmol/kg. For albumin, IgG mAb, and fibronectin, the dose used was 21.6 nmol/kg. Fifteen minutes after IgG mAb administration with or without peptide, the animals were sacrificed and PBS with 0.5% Tween-20 was administered for cardiac perfusion to remove the remaining protein in the BBB microvessels. The brain and other organs such as lung, heart, spleen, liver and kidney were harvested and rinsed with PBS. Protein depositions in the brain and other organs were quantified by NIRF imaging using an Odyssey CLx NIRF scanner.

A second quantification method was done using brain homogenates. In this case, the brains were homogenized in 2.0 mL PBS by mechanical disruption and 200 μL of homogenized brain (n = 8) was aliquoted to a 96-well plate followed by quantification using the Odyssey CLx scanner. The signal intensity was compared to calibration curve and normalized to brain weight and homogenate volume.

Brain Perfusion.

After euthanasia using CO_2 chamber, mice were immediately subjected to cervical dislocation followed by removal of IRdye800CW-labeled protein from the brain capillaries using perfusion solution. In this case, a solution containing PBS with 0.2% Tween-20 was transcardially perfused to remove the remaining protein molecules in the brain endothelial microvessels. After perfusion, the brain was removed from the skull and subjected to capillary depletion.

Capillary Depletion Method.

Parallel capillary depletion experiments were performed as described by Triguero *et al.*[26] to ensure that there was no trapping of the delivered molecules in the BBB microvessel endothelial cells. IRdye800CW-labeled protein was added and mixed into brain homogenates; then, the mixture was divided into two sets. A 500 μL set of homogenates was mixed with 500 μL of PBS while another set of 500 μL homogenates was mixed with 500 μL of 26% dextran solution. Both sets were centrifuged at 5,400 g for 15 min at 4 °C and 200 μL of supernatant was collected for analysis using the Odyssey CLx scanner.

Statistical Analysis.

The data from the brain delivery of various sized molecules were analyzed and compared using ANOVA with Student–Newman-Keuls for indication of statistical significance. The criterion for statistical significance was selected for the p-value of less than 0.05.

RESULTS

Peptide Synthesis and Purification.

The Fmoc solid-phase synthesis method was used to make linear precursor to ADTC5 and HAV6 peptides. ADTC5 was cyclized using air oxidation in a high dilution solution at pH 9.0 to give mostly the desired cyclic monomer. A semi-preparative HPLC with C18 column was used to purify both ADTC5 and HAV6 peptides with >96% purity of each peptide as determined by C18 column in analytical HPLC. The mass spectra for both purified peptides show exact masses of 650.2869 Da for sodium adduct of HAV6 and 795.2778 Da for sodium adduct of ADTC5 (Table 1).

Synthesis and Purification of IRdye800CW-labeled Proteins.

To make IRdye800CW-labeled lysozyme, albumin, or fibronectin, IRdye800CW-NHS was reacted to free amino groups of the respective protein to form stable conjugates. To purify the protein conjugates, the excess of IRdye800CW-NHS was removed from the reaction mixture using a Pierce Zeba desalting spin column with a cut-off molecular weight of 7 kDa. The purified conjugates were evaluated with SDS-PAGE scanned with an Odyssey CLx NIR imager. Lysozyme and albumin conjugates showed a single band while fibronectin had a faint lower fragment band; all proteins have the appropriate mass without unreacted IRdye (Figure 1). The final protein concentrations for lysozyme, albumin, and fibronectin were determined to be 1.35, 1.68, 2.30 mg/mL, respectively.

Initial Brain Delivery of IRDye800CW-IgG mAb by ADTC5 in SJL/Elite Mice.

In this study, IgG mAb was administered via i.v. in SJL/elite mice in the absence or presence of ADTC5 peptide. Prior to injection, IgG mAb identity was evaluated using SDS-PAGE gel and showed a major band at ~150 kDa with very light bands for ~100 kDa heavy and ~50 kDa light chains (data not shown). There was no observation of the band for IRDye800CW alone. To remove the excess IgG mAb from the brain capillaries, the mice were perfused with PBS + Tween-20 perfusion solution. After brain extraction, the brain scans of mice treated with IgG mAb alone showed very low NIRF image in eight different levels of brain scans (n = 4) (Figure 2A). In contrast, the mouse brains administered with IgG mAb and ADTC5 showed strong NIRF signals on eight different brain scan levels (n = 5) (Figure 2A). Quantitative accumulation of NIRF signals from all scan levels indicated that the brains from mice treated with IgG mAb + ADTC5 had a significantly higher signal intensity than those of mice treated with IgG mAb alone (Figure 2B). In summary, ADTC5 increases the brain delivery of IgG mAb in C57BL/6 mice.

Method Development and Validation of NIRF Quantification.

Linearity, Accuracy, and Precision.—The lowest limit of detection (LLOD) and intra-day as well as inter-day precision and accuracy were determined using a calibration curve generated with concentrations from 0.5 to 50 ng/mL (Table 2). The calibration curve was generated by plotting concentrations of standard *vs.* NIRF intensity from the Odyssey CLx imaging system (Figure 3). The resulting standard curve has good linearity with $R^2 \geq 0.98$ and LLOD of 0.3 ng/mL. Three different protein concentrations were used to determine

intra-day and inter-day accuracy and precision and for obtaining %RSD and %RE (Table 2). The acceptable analytical method was determined when the %RSD and %RE values were less than 15%.

Stability Assay.—The stability of the analyte during evaluation was investigated using IRDye800CW-lysozyme in three concentrations at two temperatures and a freeze-thaw condition (Table 3); in different analyte concentrations, the %RSD was less than 15% at room temperature for 6 h. Thus, this condition was used in this study. In contrasts, the two other conditions were determined to be unacceptable for this study because the %RSD was higher than 15%.

Comparison of HAV6 and ADTC5 in Enhancing Brain Delivery of Various Proteins.

In this study, the activities of HAV6 and ADTC5 peptides to deliver various sized proteins (*i.e.,* lysozyme, albumin, IgG mAb, and fibronectin) in C57BL/6 mice were compared in a quantitative manner. The intensities of lysozymes at various concentrations in the brain homogenates are shown in Figure 2A. Figure 2A also shows the examples of NIRF scans of brain homogenates from animals treated with lysozyme alone, lysozyme + HAV6, and lysozyme + ADTC5. The resulting calibration curve generated from 0.5 to 50 ng/mL of lysozyme produced a linear curve with $R^2 \geq 0.99$ (Figure 2B). Similar calibration curves were generated for albumin and IgG mAb. The amount of protein in the brain was determined by interpolation of NIRF intensity of the brain homogenate into the standard curve.

Brain Delivery of 15 kDa Lysozyme and Peripheral Organ Distributions.—The first delivery of lysozyme was carried out at a dose of 21.6 nmol/kg with 13 μmol/kg of HAV6 or ADTC5 peptide, and no significant improvement was observed in the brain compared to lysozyme alone (data not shown). Next, the dose of lysozyme was increased to 54 nmol/kg with 13 μmol/kg of HAV6 or ADTC5 peptide (Figure 4). Prior to brain extraction for NIRF imaging, the mice were perfused to remove the remaining lysozyme in the brain capillaries. Through visual observation, the NIRF brain images of mice treated with HAV6 + lysozyme and ADTC5 + lysozyme appeared to show higher intensity than those treated with lysozyme alone (Figure 4A). The NIRF intensity of the ADTC5 group was higher than that of HAV6 group. Quantitatively, the average amount of lysozyme in the ADTC5 group (37.8 ± 7.1 pmol/g brain) was significantly higher than that in the HAV6 group (8.3 ± 2.5 pmol/g brain, $p < 0.05$) (Figure 4B, Table 4). The lysozyme amounts in the brains of both peptide groups were higher than that of control group, which was below the detection limits. The results suggest that ADTC5 is a better BBB modulator than HAV6. To ensure that the brain perfusion procedure eliminated any residual molecule in the BBB microvessels, the brain capillary depletion was carried out using the brain homogenates. The capillary depleted samples were compared to non-depleted samples. The difference between the capillary depleted and non-depleted samples was less than 1.9%, indicating the that the perfusion method was satisfactory in removing almost all the labeled protein from the brain capillaries.

The effects of HAV6 and ADTC5 in lysozyme distributions in kidney, lung, heart, spleen, and liver were also determined. Visually, the most intense NIRF images were in the kidney in all three groups, with the highest image intensity on ADTC5 group (Figure 4C). Quantitative data confirmed that lysozyme deposition in the kidney was the highest in the ADTC5-treated group, followed by the HAV6-treated group and control (Figure 4D). It is not surprising that the lysozyme undergoes glomerular filtration in the kidney because of its molecular weight being lower than 65 kDa.

Brain Delivery of 65 kDa Albumin and Peripheral Organ Distributions.—To evaluate molecules larger than lysozyme, 65 kDa albumin was delivered using HAV6 and ADTC5 in C57BL/6 mice compared to control (*i.e.,* albumin alone) (Figures 5A, B). The calibration curve was generated with 0.5 to 500 ng/mL labeled albumin in brain homogenates to generate a good linearity with $R^2 \geq 0.98$. Prior to quantification of albumin deposition, the brains were subjected to perfusion process to remove the remaining albumin in the brain microvessels. The mice treated with albumin + ADTC5 showed a significantly higher albumin deposition (40.7 ± 7.4 pmol/g brain) compared to albumin alone (11.8 ± 1.0 pmol/g; $p < 0.05$). Although it was not significant, the HAV6 group showed a trend of enhanced brain with brain deposition of 15.5 ± 3.1 pmol/g compared to control (11.8 ± 1.0 μmol/g brain ($p = 0.20$)). These data also showed that ADTC5 was a better BBB modulator than HAV6 in delivering albumin.

The effects of HAV6 and ADTC5 peptides in the distribution of albumin in different organs were evaluated using NIRF quantitative imaging (Figures 5C, D). The data indicated that HAV6 ($p = 0.04$) and ADTC5 ($p = 0.04$) significantly enhanced the distributions of albumin into the liver compared to control. There was no significant difference in albumin depositions between the liver ADTC5 group and the HAV6 group ($p = 0.15$). Although the deposition in spleen is lower than in liver, the HAV5 and ADTC5 groups both enhanced the deposition of albumin in the spleen compared to control.

Brain Delivery of 150 kDa IgG mAb and Peripheral Organ Distributions.—Because many mAbs have been utilized as therapeutics, there is high interest in improving their brain delivery. For quantitative determinations, a calibration curve for mAb was prepared with concentrations ranging from 10 to 200 ng/mL of IRDye800CW-IgG mAb spiked into blank brain homogenates. The calibration curve showed good linearity with $R^2 \geq 0.99$. The mice were perfused to remove any residual IgG mAb in the brain capillaries to avoid additional NIRF signal from protein in the capillaries. As in the previous study in SJL/elite, NIRF imaging signals from mAb in the brains of ADTC5 + mAb-treated mice were higher than those of mAb-treated mice in C57BL/6 mice (Figure 6A). The amounts of mAb in the brains of mice treated with ADTC5 + mAb (13.3 ± 0.7 pmol/g) were significantly higher compared to those of HAV6 + mAb (3.42 ± 0.5 pmol/g; $p < 0.05$) and mAb alone (4.0 ± 0.4 pmol/g; $p < 0.05$; Figure 6B). HAV6 peptide was not able to deliver mAb ($p > 0.05$) compared to control mAb (Figure 6B). The enhancement of mAb brain deposition by ADTC5 is about three times that of control. ADTC5 showed a trend to enhance the distribution of mAb into liver compared to HAV6- ($p = 0.06$) and control-treated animals

($p = 0.06$) (Figures 6C, D). The distributions of mAb in HAV6- and control-treated animals were about the same ($p = 0.54$).

Brain Delivery of 220 kDa Fibronectin and Peripheral Organ Distributions.—To find the larger limit of pore sizes made by ADTC5 peptide, the brain delivery of fibronectin (220 kDa) was evaluated in the presence and absence of ADTC5 (Figure 7A, B). HAV6 was not investigated for delivering 220 kDa fibronectin because it cannot deliver 150 kDa mAb. ADTC5 did not enhance brain delivery of 220 kDa fibronectin because the NIRF signals for the ADTC5 + fibronectin group ($35.498 \pm 3.001 \times 10^3$A.U.) was not different than that of fibronectin alone group ($33.026 \pm 2.080 \times 10^3$ A.U.) (Figure 7A, B). The distributions of fibronectin were mostly in the liver, and ADTC5 did not influence the distribution of fibronectin in other organs (Figure 7C, D).

DISCUSSION

Proteins have been successfully used to treat many diseases, and some proteins such as mAbs have been evaluated to treat brain diseases such as brain tumors (*e.g.,* glioblastoma) as well as neurodegenerative diseases, including Alzheimer's, multiple sclerosis (MS), and Parkinson's. Unfortunately, many proteins, including mAbs that were developed to treat brain diseases, have failed in clinical trials. One of the reasons is the inefficiency of proteins to cross the BBB sufficiently to exude their activities in the brain. The BBB plays a vital role in restricting unwanted molecules from reaching the brain for regulating the internal environment of the brain.[27] Various approaches have been investigated to deliver drugs to the brain following systemic administration. Our approach is to use cadherin peptides to modulate cadherin-cadherin interactions to create larger pores in the intercellular junctions to allow proteins to enter the brain in a non-invasive manner. In an initial proof-of-concept, ADTC5 peptide was used to deliver IRDye800CW-IgG mAb in SJL/elite mice. The brains of animals treated with ADTC5+IgG mAb had high NIRF intensities while very low NIRF intensities were observed in the brains of animals treated with IgG mAb alone (Figure 2). With the initial data, the next step was to compare the effectiveness of HAV6 and ADTC5 peptides in enhancing the brain delivery of various sized proteins such as 15 kDa lysozyme, 65 kDa albumin, 150 kDa IgG mAb, and 220 kDa fibronectin. It was proposed that each peptide has different BBB modulatory activities in delivering different sizes of proteins. In addition, each peptide creates a maximum pore size opening in the paracellular pathway so there is a cut-off size of proteins that can pass through the BBB. Thus, it was necessary to develop a rapid method to quantitatively determine the amount of protein delivered into the brain. Finally, the effects of each peptide on the distributions of i.v. administered proteins in organs other than the brain were evaluated.

Prior to evaluating the delivery of various sized proteins, 150 kDa IR800-IRdye-IgG mAb was administered via i.v. tail-vein injection to SJL/elite mice in the presence (n = 5) and absence (n = 4) of ADTC5 peptide (13 μmol/kg) and allowed to circulate for 15 min (Figure 2). The brains of mice administered mAb alone (n = 4) showed very low background-intensity NIRF (Figure 2A, left images), suggesting that little or no mAb entered the brain. The brains of mice administered mAb + ADTC5 showed high NIRF intensity, suggesting that ADTC5 enhanced mAb brain delivery (Figure 2A, right images). The mean pixel

NIRF intensity was significantly higher (4.7 times higher) in mAb + ADTC5-treated mice compared to those from mice injected with mAb alone (Figure 2B). Because IgG mAb can be delivered to the brain, a NIRF quantitative method was developed to determine the amounts of delivered proteins in the brain per gram of brain (pmol/g brain).

To develop a simple, rapid, and quantitative method to determine the amount delivered protein in the brain, NIRF imaging method was used in this study. Calibration curves were developed for each delivered protein. Homogenized brain samples were spiked with different concentrations of standard labeled proteins, and fluorescence intensities were determined using with the Odyssey CLx scanner (Figure 3A). Good linearity for the calibration curve was achieved with $R^2 \geq 0.98$. The amount of delivered protein in the brain in pmol/g brain can be determined by interpolating the NIRF intensity from the brain homogenate into the calibration curve (Figure 3B). The NIRF method was validated using IRDye800CW-lysozyme QC samples; in this case, the stability, accuracy, and precision were determined over the range of calibration curve as suggested by FDA guidelines.[27] Thus, less than 15% RSD and RE for intra-day and inter-day precision and accuracy variability were taken to be accurate and precise for the NIRF method (Table 2). Only the brain homogenates that were kept at room temperature for 6 h showed %RSD values under 15%; thus, this condition was used for all analyses. In contrast, the other two conditions were deemed to be unstable for the protein in brain extracts. Therefore, all the analyses were done within the time frame of 6 h. With a linear calibration curve and lower %RSD and %RE values for precision and accuracy, the developed NIRF imaging method was very sensitive and reliable for detecting and quantifying the delivered labeled proteins.

To carry out the *in vivo* brain delivery experiments, the protein was administered via i.v. with and without BBB modulators (*i.e.,* HAV6 or ADTC5) followed by allowing the delivered protein to remain in the systemic circulation for 15 min. The animal was then euthanized, followed by perfusion of the brain capillaries to eliminate the remaining protein in the blood vessels. In addition, capillary depletion experiments were performed to check whether the optimized perfusion procedure removed the residual IRdye800CW-labeled proteins from the microvessel endothelial cells in the brain that could create false positives. For IRdye800CW-lysozyme, there was 1.9% difference in the quantitation of lysozyme in the brains with and without capillary depletion. This result suggests that the perfusion method was effective in removing the residual protein from the brain capillaries. In addition, during brain delivery of 220 kDa fibronectin, the NIRF fluorescence images of the brain did not show any signal of IRdye800CW-fibronectin that show brain capillaries delivered with and without ADTC5. This results also support that the perfusion method removed fibronectin from the brain microvessels. To quantify the protein deposition, the brain was isolated and homogenized followed by transferring the homogenates into a 96-well plate. The intensity of NIRF from the protein in the homogenate was detected by scanning with the Odyssey CLx scanner and the intensity was normalized by weight of the brain. Previously, the NIRF method has been used to quantify study IRDye800CW mAb distribution *ex vivo* in tissues. The method was deemed to be accurate and sensitive when compared to a commonly used reference method called gamma ray quantification.[28] Comparison of NIRF and gamma ray quantification data sets using the Bland-Altman method concluded that the results from quantification using NIRF are the same as those using the gamma ray method.[28]

Comparison between the activities of ADTC5 and HAV6 in modulating the BBB provides insight into the paracellular pore size openings and potential use of each peptide in delivering various sized proteins into the brain. In this study, ADTC5 peptide can effectively improve the delivery of lysozyme, albumin, and IgG mAb into the brains compared to control; however, ADTC5 cannot enhance the delivery of 220 kDa fibronectin. Using a 15-min circulation time, the results suggest that ADTC5 created pores large enough to allow proteins with the largest size between 150 and 220 kDa to penetrate the BBB. Using the same experimental conditions, HAV6 significantly enhanced the brain delivery of lysozyme but not albumin and IgG mAb, indicating that the pore-size opening in the BBB paracellular pathways was smaller than that crated by ADTC5. In summary, the modulatory activity of ADTC5 is distinctly different than that of HAV6; thus, this difference can be used to deliver selected groups of proteins, depending on the therapeutic need.

Although lysozyme is smaller than albumin and IgG mAb, no observable lysozyme was found in the brains when delivered with a dose of 21.6 nmol/kg along with HAV6 or ADTC5 at 13 μmol/kg (data not shown). In contrast, the lysozyme was observed in the brain when it was delivered at a higher dose (54 nmol/kg) along with HAV6 or ADTC5 at 13 μmol/kg (Figure 4). The depositions of lysozyme were significantly higher in the brain when delivered with ADTC5 compared to HAV6 peptide (Figure 4A, B). In addition, the amounts of lysozyme in the brains were slightly lower than albumin when delivered using HAV6 or ADTC5, although the administered dose of lysozyme was higher than that of albumin (Table 4). One of the explanations for the need of a higher dose of lysozyme is the rapid clearance of lysozyme in the kidney because of glomerular filtration. The depositions of lysozyme in the kidney were higher than in other organs (*i.e.,* heart, lung, spleen, and liver) (Figures 4C, D). It is interesting to find that ADTC5-treated mice have significantly enhanced deposition of lysozyme in the kidney compared to control, suggesting that ADTC5 affected cadherin interactions in the kidney. In contrast, HAV6 did not significantly enhance the amount of lysozyme in the kidney compared to control. Previously, low molecular weight proteins (LMWP) have been shown to be suitable carriers for specific renal drug delivery due to their high accumulation in kidney. They are freely filtered in the glomerulus and subsequently accumulate specifically in the proximal tubular cells, utilizing receptor-mediated endocytosis.[29, 30] Conjugation of the antihypertensive drug captopril and the analgesic drug naproxen to lysozyme resulted in a 6–to–60-fold enriched accumulation in the kidney.[31] Taken together, the results suggest that the brain delivery of lysozyme or other proteins is influenced by its kidney clearance, resulting in a decrease in systemic concentration for penetration into the brain.

Albumin has been explored as a drug carrier where several strategies have been developed including various forms of physical and covalent binding (*e.g.,* albumin-drug and peptide conjugate) as well as drug encapsulation in albumin nanoparticles.[15, 32–34] Falcone *et al.* showed an improved brain uptake of radioactive-labeled albumin in CD1 mice when administered via intranasal delivery;[15] however, there is no clear mechanism for the way that albumin can be transported into the brain. The paracellular brain delivery of albumin using ADTC5 and HAV6 was compared and quantified by NIRF imaging. It showed a significantly higher brain deposition of albumin in the presence of ADTC5 compared to control and HAV6 peptide (Figure 5A, B). In contrast, the HAV6-treated group did not have

significantly higher brain deposition of albumin compared to a control group (*i.e.,* albumin alone). Although, using the current conditions, HAV6 peptide did not enhance the delivery of albumin, our previous data showed that HAV6 peptide could significantly enhance the delivery of 65 kDa galbumin (a gadolinium complex conjugated to albumin) into the brain compared to control as detected using magnetic resonance imaging (MRI) in living mice.[22] In the MRI study, the dose of HAV6 peptide (10 μmol/kg) was similar to the current study dose, but the dose of galbumin in the MRI study was 27 times higher (600 nmol/kg) than the dose (21.6 nmol/kg) in the current study.[22] The circulation time of the MRI study was 51 min compared to 15 min in the current study. Therefore, the high dose of galbumin provides a more pronounce amount of galbumin in the brain as detected by MRI. The MRI studies suggested that ADTC5 was a better enhancer of galbumin brain delivery than HAV6, and this previous finding was confirmed by the current findings when ADTC5 was compared to HAV6 in delivering IRdye800CW-albumin (Table 4). ADTC5 significantly enhanced brain deposition of albumin while HAV6 did not (Figure 5A, B). In summary, the data indicated that ADTC5 is a better modulator for large proteins compared to HAV6 peptide, and the dose of delivered molecules influences the transport of molecule across the BBB. The results also suggest that both peptides created different populations of small, medium, and large pore sizes, but ADTC5 created a higher population of large pores than did HAV6 peptide. Thus, ADTC5 allows larger molecules to penetrate the BBB compared to HAV6.

The enhancement of IgG mAb brain delivery using ADTC5 or HAV6 was evaluated. Due to their size, passive diffusion of IgG mAb across the BBB was very minimal and normally antibody brain concentrations are 1,000 times lower than in the bloodstream. Here, brain delivery of IgG mAb was significantly improved by ADTC5 in C57BL/6 mice but not by HAV6 (Figure 5A, B; Table 4). The results support a proposal that each peptide has a limit of size cut-off for delivering various sized proteins. In the future, the effects of circulation time and multiple injections of proteins will be explored in the future to determine the optimal delivery protocol for mAbs or other proteins. This method can also be used to rapidly screen the modulatory activity of new peptides in improving brain protein delivery.

The data from mice treated with both peptides suggest that there is a cut-off size for each peptide in delivering molecules to the brain. ADTC5 peptide did not enhance the delivery of fibronectin (220 kDa), suggesting that the molecular size cut-off for ADTC5 is 220 kDa. The molecular cut-off is important to limit the number of unwanted molecules or proteins from penetrating the BBB and potentially generating side effects. It is interesting to find that both HAV6 and ADTC5 exuded BBB modulation temporarily and reversibly in a short duration. Previously, ADTC5 and HAV6 have been shown to modulate the BBB immediately, allowing delivered molecules to enter the brain within 3 min.[17, 20, 22] The modulation of the BBB by HAV6 within the span of less than 1 h would allow a small molecule such as Gd-DTPA (547 Da) to enter the brain.[20] In contrast, HAV6 did not allow 65 kDa galbumin to enter the brain after a 10-min delay between delivery of HAV6 and galbumin.[22] Pretreatment of mice with ADTC5 produced a longer opening (between 2 and 4 h) than with HAV6 for a small molecule such as Gd-DTPA.[17] However, with large molecules (*e.g.,* galbumin, 65 kDa), ADTC5 showed an enhancement only after a 10-min delay of pretreatment with peptide but no enhancement after a 40-min pretreatment.[22] The duration of paracellular pathways opening of the BBB created by ADTC5 is longer for all

types of molecules compared to HAV6.[22] For ADTC5 peptide, the BBB opening lasted for a smaller time frame for a large molecule than for a small molecule. More importantly, the BBB seals back to its original position after the clearance of the peptide, which is a crucial parameter in delivering selected proteins into the brain.[17, 22] Our previous studies using transmission electron microscopy showed that after modulation of the BBB with cadherin peptides (i.e., ADTC5) there are no detectable differences in the morphology of brain microvessel endothelial cells compared to that of unmodulated control.[17] We also found that vesicular activity appeared to be similar in both vehicle and peptide-treated mice.[17] Taken together, these results suggest that each peptide creates different mechanism of modulatory activity that translate to generation of various pore sizes in the intercellular junctions. One hypothesis is that BBB modulation by the peptide generates sub-populations of intercellular junction pores with various sizes such as small, medium, and large pores. It is proposed that the large pores collapse faster than medium and small pores and these large pores are converted to medium and small pores. Subsequently, the medium pores collapse to small pores in a time-dependent manner. Finally, the intercellular junction is resealed to the normal condition. In the future, we will investigate the kinetics of these pore conversions.

Evaluations of ADTC5 and HAV6 peptides in other organs are necessary to assess their applicability as drug delivery enhancers because cadherin-mediated cell-cell adhesion is present in other organs (*i.e.,* kidney, lung, spleen, liver, and heart). Modulation of cadherin-cadherin interactions in other organs may lead to increased permeability to other parts of the body, which can lead to off-target site delivery as well as side effects in the host. Therefore, it is necessary to find out the effects of each peptide on the deposition of delivered proteins in other organs. The results could also be utilized to design better and selective BBB modulators that will not affect other organs. As mentioned previously, 15 kDa lysozyme is highly accumulated in the kidney compared to other organs (*i.e.,* heart, spleen, lungs, and liver) for all three groups (*i.e.,* control, HAV6-, and ADTC5-treated groups). ADTC5-treated groups had significantly higher lysozyme kidney deposition compared to control while HAV6-treated groups did not. ADTC5-treated groups for all other proteins larger than lysozyme have higher deposition in the liver compared to control but lower deposition in kidney, spleen, lung, and heart. For HAV6-treated groups, only albumin has higher deposition in the liver compared to control, and there were no significant differences in other organs. There was no enhancement of fibronectin deposition in the liver of ADTC5-treated groups. In summary, ADTC5 has influenced in depositions of delivered proteins in kidney or liver while HAV6 has influence in protein deposition in kidney and liver for lysozyme and albumin, respectively.

Unlike hypertonic mannitol solution in osmotic BBB modulation, HAV6 and ADTC5 peptides modulate the BBB by selectively binding to the EC1 domain of E-cadherins to inhibit cadherin-cadherin interactions in equilibrium-type fashion. In mice *in vivo* studies, the tight junctions of the BBB that are modulated by ADTC5 had returned to normal between 2- to 4-h after treatments with ADTC5 peptide, suggesting the selective and reversible nature of the BBB opening cadherin peptides.[17] The inhibition of cadherin-cadherin interactions increases the pore size opening at the BBB intercellular junctions. We have shown that *in vivo* modulations of the BBB by HAV6 and ADTC5 are dose dependent, suggesting both peptides target cadherins on the intercellular junctions.[17, 20] NMR studies

indicated that both HAV6 and ADTC5 bind to different binding sites on the EC1 domain of E-cadherin protein.[35] To evaluate the effects of BBB modulator on brain toxicity, the influence of HAV6 in inducing brain inflammation and astrogliosis was determined by monitoring the expression upregulation of glial fibrillary acidic protein (GFAP) in astrocytes and ionized calcium binding adaptor molecule 1 (Iba1) in microglia.[24] The brains of mice treated with HAV6 did not show increased expressions of either GFAP and Iba1, suggesting that there were no inflammation and astrogliosis due to HAV6 treatments. Iba1 upregulation has been used as indicator for CNS inflammation due to microglia and macrophage activation. GFAP is a marker of astrogliosis due stimulation of astrocyte growth in neuroinflammation.[36, 37] In conclusion, modulation of the BBB by HAV6 peptide did not generate inflammation; this presumably due to short-term, reversible, selective modulation of the BBB.

Both HAV6 and ADTC5 peptides bind to the EC1 domain of E-cadherin at different binding sites as determined using heteronuclear single quantum correlation (HSQC) NMR spectroscopy and molecular docking experiments. ADTC5 binds to I4, P5, P6, S8, and P10 residues on the N-terminal β sheet of the EC1 domain while HAV6 binds to the Y36, I38, F77, S78, and I94 residues of the EC1 domain.[35] Using the X-ray structure of C-cadherin as a model, it is proposed that HAV6 peptide binds to the EC1 domain and blocks the EC1-EC2 *cis*-cadherin derived from two cadherins on the same cell membranes.[38, 39] In contrast, ADTC5 binds to the domain-swapping region of EC1 and inhibits EC1-EC1 *trans*-cadherin interactions from the opposite cells.[35] Because ADTC5 blocks *trans*-cadherin interactions, its effects on the intercellular junctions presumably are more pronounced than those of HAV6, which inhibits *cis*-cadherin interactions. Experimentally, our data for all proteins indicate that ADTC5 has higher modulatory activity and longer duration of BBB modulation than HAV6, and these observations could partly be explained by their binding mechanisms.

CONCLUSION

ADTC5 can deliver 15 kDa lysozyme, 65 kDa albumin, and 150 kDa mAb IgG but not 220 kDa into the brain of C57BL/6 mice while HAV6 can enhance only brain delivery of lysozyme. Each peptide creates cut-off size of proteins that can be delivered into the brain. HAV6 peptide only allows molecule less than 65 kDa to enter the brain while ADTC5 can deliver molecules of less than 220 kDa to enter the brain. ADTC5 and HAV6 peptides could enhance the depositions of delivered proteins in the kidney and liver. Finally, the NIRF imaging method is a very useful and rapid method to quantitively determine the amounts of delivery of proteins in the brain. In the future, we will design peptides that are more selective to the cadherins in the intercellular junctions of the BBB over the other organs.

ACKNOWLEDGMENTS

We would like to thank the National Institutes of Health (NIH) for providing us with the support through R01-NS075374 from the National Institute of Neurological Disorders and Stroke (NINDS) and P30-AG035982 from the KU Alzheimer's Disease Center-National Institute on Aging (NIA). We would like to acknowledge the T32 NIH Predoctoral Training Program on Pharmaceutical Aspects of Biotechnology (T32-GM008359) that supported BMK as a trainee. We are grateful to Nancy Harmony for proofreading this manuscript.

REFERENCES

1. Tomlinson IM Next-generation protein drugs. Nature Biotechnology 2004, 22, 521.
2. Numakawa T; Suzuki S; Kumamaru E; Adachi N; Richards M; Kunugi H BDNF function and intracellular signaling in neurons. Histol Histopathol 2010, 25, (2), 237–58. [PubMed: 20017110]
3. Masoudi R; Ioannou MS; Coughlin MD; Pagadala P; Neet KE; Clewes O; Allen SJ; Dawbarn D; Fahnestock M Biological activity of nerve growth factor precursor is dependent upon relative levels of its receptors. J Biol Chem 2009, 284, (27), 18424–33. [PubMed: 19389705]
4. Apel PJ; Ma J; Callahan M; Northam CN; Alton TB; Sonntag WE; Li Z Effect of locally delivered IGF-1 on nerve regeneration during aging: an experimental study in rats. Muscle Nerve 2010, 41, (3), 335–41. [PubMed: 19802878]
5. Laksitorini M; Prasasty VD; Kiptoo PK; Siahaan TJ Pathways and progress in improving drug delivery through the intestinal mucosa and blood-brain barriers. Ther Deliv 2014, 5, (10), 1143–63. [PubMed: 25418271]
6. Kiptoo P; Laksitorini MD; Siahaan TJ, Blood-Brain Peptides: Peptide Delivery. In Handbook of Biologically Active Peptides, Kastin A, Ed. Academic Press: Boston, 2013; pp 1702–1710.
7. Bickel U; Yoshikawa T; Pardridge WM Delivery of peptides and proteins through the blood-brain barrier. Adv Drug Deliv Rev 2001, 46, (1–3), 247–79. [PubMed: 11259843]
8. Carter PJ; Lazar GA Next generation antibody drugs: pursuit of the ‘high-hanging fruit’. Nat Rev Drug Discov 2018, 17, (3), 197–223. [PubMed: 29192287]
9. Ineichen BV; Plattner PS; Good N; Martin R; Linnebank M; Schwab ME Nogo-A Antibodies for Progressive Multiple Sclerosis. CNS Drugs 2017, 31, (3), 187–198. [PubMed: 28105588]
10. Ruggieri S; Tortorella C; Gasperini C Anti lingo 1 (opicinumab) a new monoclonal antibody tested in relapsing remitting multiple sclerosis. Expert Rev Neurother 2017, 17, (11), 1081–1089. [PubMed: 28885860]
11. Ciric B; Howe CL; Paz Soldan M; Warrington AE; Bieber AJ; Van Keulen V; Rodriguez M; Pease LR Human monoclonal IgM antibody promotes CNS myelin repair independent of Fc function. Brain Pathol 2003, 13, (4), 608–16. [PubMed: 14655764]
12. Fisher TL; Reilly CA; Winter LA; Pandina T; Jonason A; Scrivens M; Balch L; Bussler H; Torno S; Seils J; Mueller L; Huang H; Klimatcheva E; Howell A; Kirk R; Evans E; Paris M; Leonard JE; Smith ES; Zauderer M Generation and preclinical characterization of an antibody specific for SEMA4D. MAbs 2016, 8, (1), 150–62. [PubMed: 26431358]
13. Lipinski CA Lead- and drug-like compounds: the rule-of-five revolution. Drug Discov Today Technol 2004, 1, (4), 337–41. [PubMed: 24981612]
14. Kobus T; Zervantonakis IK; Zhang Y; McDannold NJ Growth inhibition in a brain metastasis model by antibody delivery using focused ultrasound-mediated blood-brain barrier disruption. J Control Release 2016, 238, 281–288. [PubMed: 27496633]
15. Falcone JA; Salameh TS; Yi X; Cordy BJ; Mortell WG; Kabanov AV; Banks WA Intranasal administration as a route for drug delivery to the brain: evidence for a unique pathway for albumin. J Pharmacol Exp Ther 2014, 351, (1), 54–60. [PubMed: 25027317]
16. Neuwelt EA; Barnett PA; Hellstrom I; Hellstrom KE; Beaumier P; McCormick CI; Weigel RM Delivery of melanoma-associated immunoglobulin monoclonal antibody and Fab fragments to normal brain utilizing osmotic blood-brain barrier disruption. Cancer Res 1988, 48, (17), 4725–9. [PubMed: 3409213]
17. Laksitorini MD; Kiptoo PK; On NH; Thliveris JA; Miller DW; Siahaan TJ Modulation of intercellular junctions by cyclic-ADT peptides as a method to reversibly increase blood-brain barrier permeability. J Pharm Sci 2015, 104, (3), 1065–75. [PubMed: 25640479]
18. Doolittle ND; Muldoon LL; Culp AY; Neuwelt EA Delivery of chemotherapeutics across the blood-brain barrier: challenges and advances. Adv Pharmacol 2014, 71, 203–43. [PubMed: 25307218]
19. Kiptoo P; Sinaga E; Calcagno AM; Zhao H; Kobayashi N; Tambunan US; Siahaan TJ Enhancement of drug absorption through the blood-brain barrier and inhibition of intercellular tight junction resealing by E-cadherin peptides. Mol. Pharm 2011, 8, (1), 239–49. [PubMed: 21128658]

20. On NH; Kiptoo P; Siahaan TJ; Miller DW Modulation of blood-brain barrier permeability in mice using synthetic E-cadherin peptide. Mol Pharm 2014, 11, (3), 974–81. [PubMed: 24495091]
21. Tabanor K; Lee P; Kiptoo P; Choi IY; Sherry EB; Eagle CS; Williams TD; Siahaan TJ Brain Delivery of Drug and MRI Contrast Agent: Detection and Quantitative Determination of Brain Deposition of CPT-Glu Using LC-MS/MS and Gd-DTPA Using Magnetic Resonance Imaging. Mol Pharm 2016, 13, (2), 379–90. [PubMed: 26705088]
22. Ulapane KR; On N; Kiptoo P; Williams TD; Miller DW; Siahaan TJ Improving Brain Delivery of Biomolecules via BBB Modulation in Mouse and Rat: Detection using MRI, NIRF, and Mass Spectrometry. Nanotheranostics 2017, 1, (2), 217–231. [PubMed: 28890866]
23. Alaofi A; On N; Kiptoo P; Williams TD; Miller DW; Siahaan TJ Comparison of Linear and Cyclic His-Ala-Val Peptides in Modulating the Blood-Brain Barrier Permeability: Impact on Delivery of Molecules to the Brain. J Pharm Sci 2016, 105, (2), 797–807. [PubMed: 26869430]
24. Sajesh BV; On NH; Omar R; Alrushaid S; Kopec BM; Wang W-G; Sun H-D; Lillico R; Lakowski TM; Siahaan TJ; Davies NM; Puno P-T; Vanan MI; Miller DW Validation of Cadherin HAV6 Peptide in the Transient Modulation of the Blood-Brain Barrier for the Treatment of Brain Tumors. Pharmaceutics 2019, 11, 481.
25. Yang S; Chen Y; Feng M; Rodriguez L; Wu JQ; Wang MZ Improving eflornithine oral bioavailability and brain uptake by modulating intercellularjunctions with an E-cadherin peptide. J. Pharm. Sci 2019, 9, 20.
26. Triguero D; Buciak J; Pardridge WM Capillary depletion method for quantification of blood-brain barrier transport of circulating peptides and plasma proteins. Journal of neurochemistry 1990, 54, (6), 1882–8. [PubMed: 2355231]
27. DoHaH S; FaD A; CfDEaR C; CfBEaR C Analytical Procedures and Methods Validation for Drugs and Biologics: Guidance for Industry. Pharmaceutical Quality/CMC. 2015, 7, 1–15.
28. Oliveira S; Cohen R; Walsum MS; van Dongen GA; Elias SG; van Diest PJ; Mali W; van Bergen En Henegouwen PM A novel method to quantify IRDye800CW fluorescent antibody probes ex vivo in tissue distribution studies. EJNMMI research 2012, 2, (1), 50. [PubMed: 23009555]
29. Haas M; Kluppel AC; Wartna ES; Moolenaar F; Meijer DK; de Jong PE; de Zeeuw D Drug-targeting to the kidney: renal delivery and degradation of a naproxen-lysozyme conjugate in vivo. Kidney Int 1997, 52, (6), 1693–9. [PubMed: 9407519]
30. Haverdings RFG; Haas M; Greupink AR; deVries PAM; Moolenaar F; de Zeeuw D; Meijer DKF Potentials and Limitaitons of the Low-Molecular-Weight Protein Lysozyme as a Carrier for Renal Drug Targeting. Renal Failure 2001, 23, (3–4), 397–409. [PubMed: 11499555]
31. Kok RJ; Grijpstra F; Walthuis RB; Moolenaar F; de Zeeuw D; Meijer DK Specific delivery of captopril to the kidney with the prodrug captopril-lysozyme. J Pharmacol Exp Ther 1999, 288, (1), 281–5. [PubMed: 9862782]
32. Kratz F Albumin as a drug carrier: design of prodrugs, drug conjugates and nanoparticles. J Control Release 2008, 132, (3), 171–83. [PubMed: 18582981]
33. Kratz F; Elsadek B Clinical impact of serum proteins on drug delivery. J Control Release 2012, 161, (2), 429–45. [PubMed: 22155554]
34. Lin T; Zhao P; Jiang Y; Tang Y; Jin H; Pan Z; He H; Yang VC; Huang Y Blood–Brain-Barrier-Penetrating Albumin Nanoparticles for Biomimetic Drug Delivery via Albumin-Binding Protein Pathways for Antiglioma Therapy. ACS Nano 2016, 10, (11), 9999–10012. [PubMed: 27934069]
35. Alaofi A; Farokhi E; Prasasty VD; Anbanandam A; Kuczera K; Siahaan TJ Probing the interaction between cHAVc3 peptide and the EC1 domain of E-cadherin using NMR and molecular dynamics simulations. J Biomol Struct Dyn 2017, 35, (1), 92–104. [PubMed: 26728967]
36. Lossinsky AS; Vorbrodt AW; Wisniewski HM Scanning and transmission electron microscopic studies of microvascular pathology in the osmotically impaired blood-brain barrier. J Neurocytol 1995, 24, (10), 795–806. [PubMed: 8586999]
37. Salahuddin TS; Johansson BB; Kalimo H; Olsson Y Structural changes in the rat brain after carotid infusions of hyperosmolar solutions. An electron microscopic study. Acta neuropathologica 1988, 77, (1), 5–13. [PubMed: 3149121]
38. Wheelock MJ; Shintani Y; Maeda M; Fukumoto Y; Johnson KR Cadherin switching. Journal of cell science 2008, 121, (6), 727. [PubMed: 18322269]

39. Angst BD; Marcozzi C; Magee AI The cadherin superfamily: diversity in form and function. Journal of cell science 2001, 114, (Pt 4), 629–41. [PubMed: 11171368]

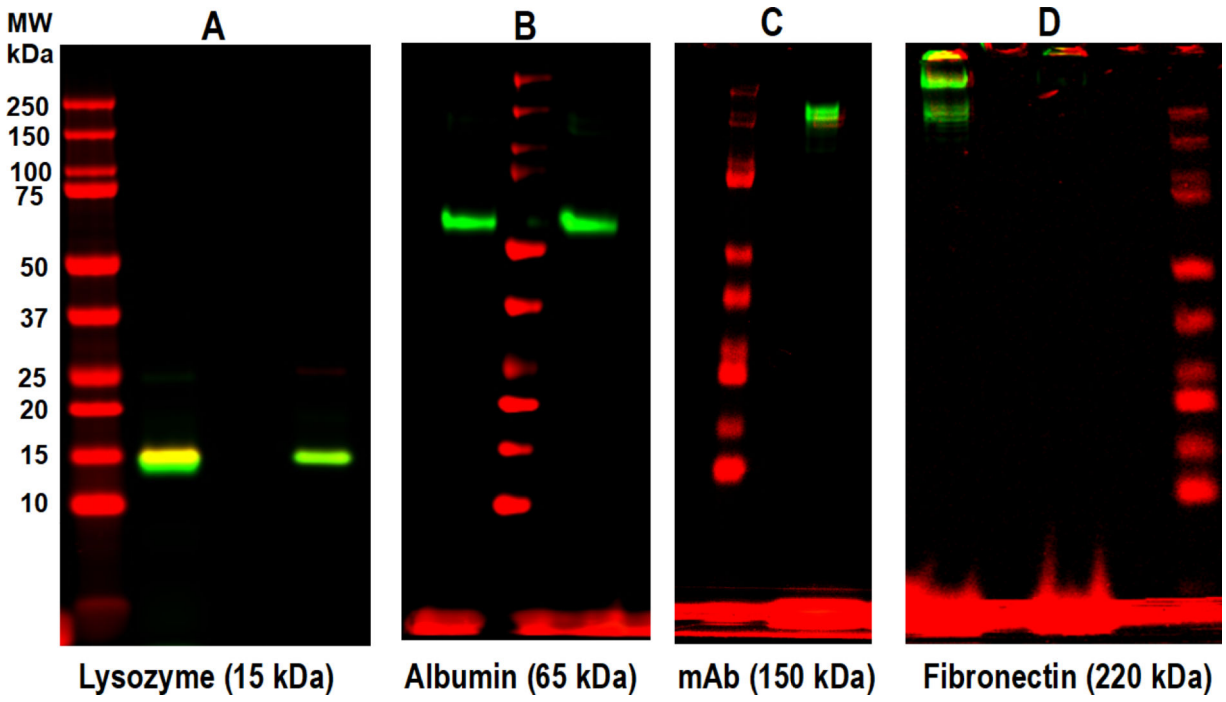

Figure 1.

SDS PAGE gels IRdye800CW-labeled (A) 15 kDa lysozyme, (B) 65 kDa albumin, (C) 150 kDa IgG mAb, and (D) 220 kDa fibronectin that are imaged using an Odyssey CLx imaging system to determine protein purity and the absence of unconjugated IRdy800cw.

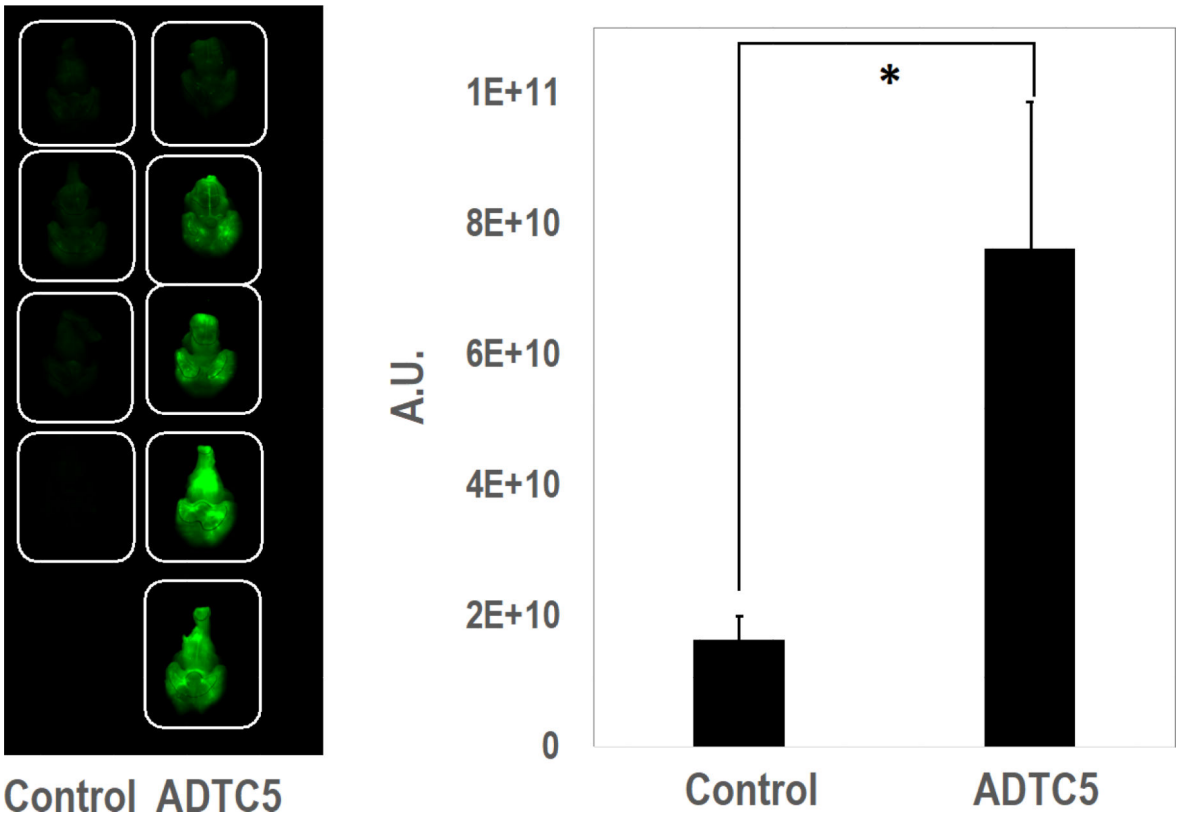

Figure 2.

The effect of ADTC5 (13 μmol/kg) on improving the brain delivery of IRdye800CW-IgG mAb (26.8 nmol/kg) in SJL/elite mice. **(A)** The image shows whole brain fluorescent of mice that received IRDye800cw-IgG mAb alone (left; n = 4) and IRDye800cw-IgG mAb + ADTC5 (right; n = 5). **(B)** Mean fluorescence intensity of IRDye800cw-IgG mAb for quantitative comparison of NIRF signals between mice that received IRDye800cw-IgG mAb+ADTC5 *vs.* IRDye800cw-IgG mAb alone. Asterisk (*) was used to designate a significant difference between the ADTC5 group and the control group when $p < 0.05$. Error bars show the mean ± SE for both groups.

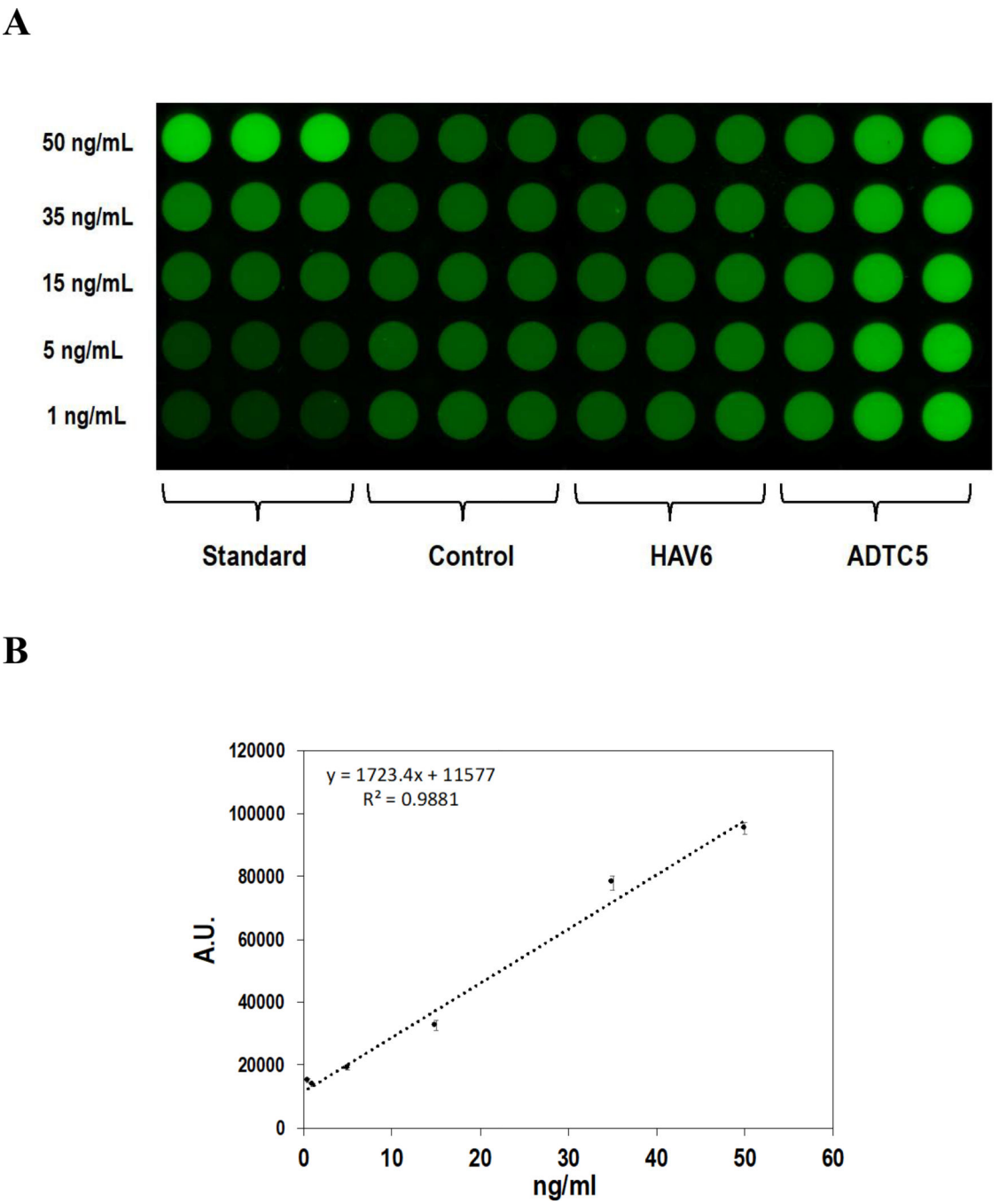

Figure 3.

Development of the quantification method and standard curve for IRdye800CW-lysozyme using NIRF image of brain homogenates in a 96-well plate scanned using Odyssey CLx imaging system. **(A)** Examples of scanned images of brain homogenates from various concentrations of standard samples as well as samples from HAV6- and ADTC5-treated mice. Each well was scanned to obtain the NIRF intensity. **(B)** An example of calibration curve for lysozyme (R = 0.988) was generated by plotting the concentrations of spiked standard against the fluorescence intensity. The concentrations of lysozyme in the brains

of HAV6- and ADTC5-treated mice were determined by interpolating the fluorescence intensity in the standard curve.

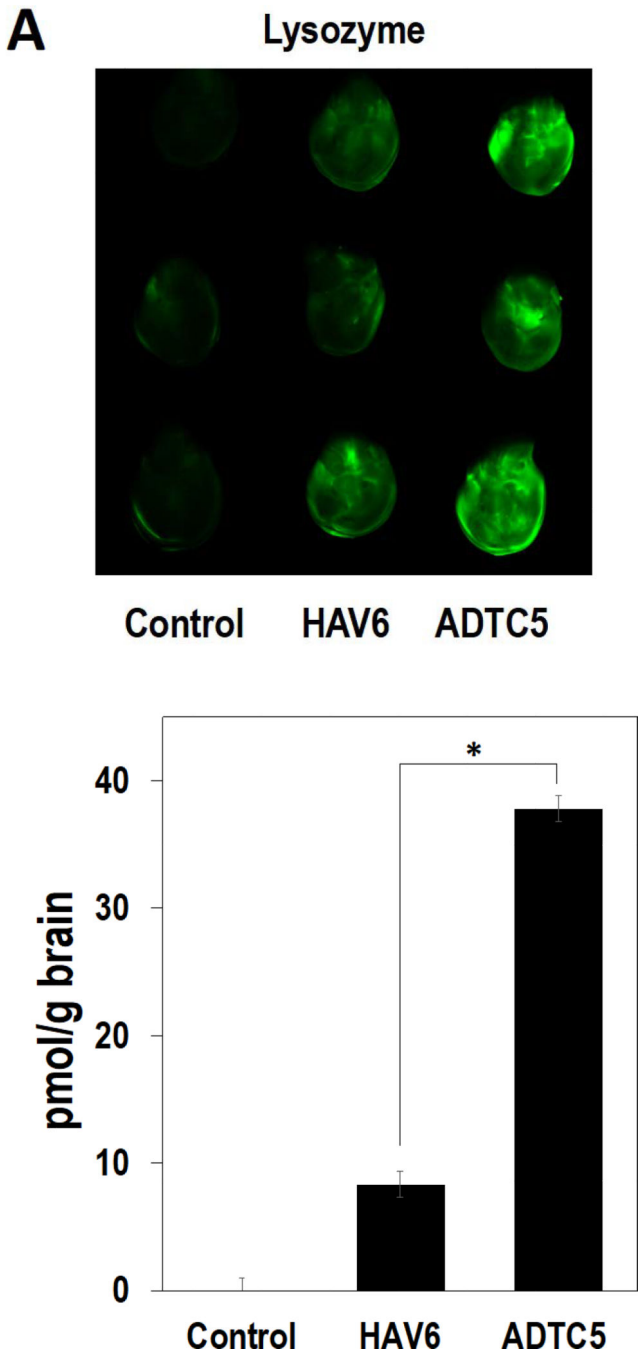

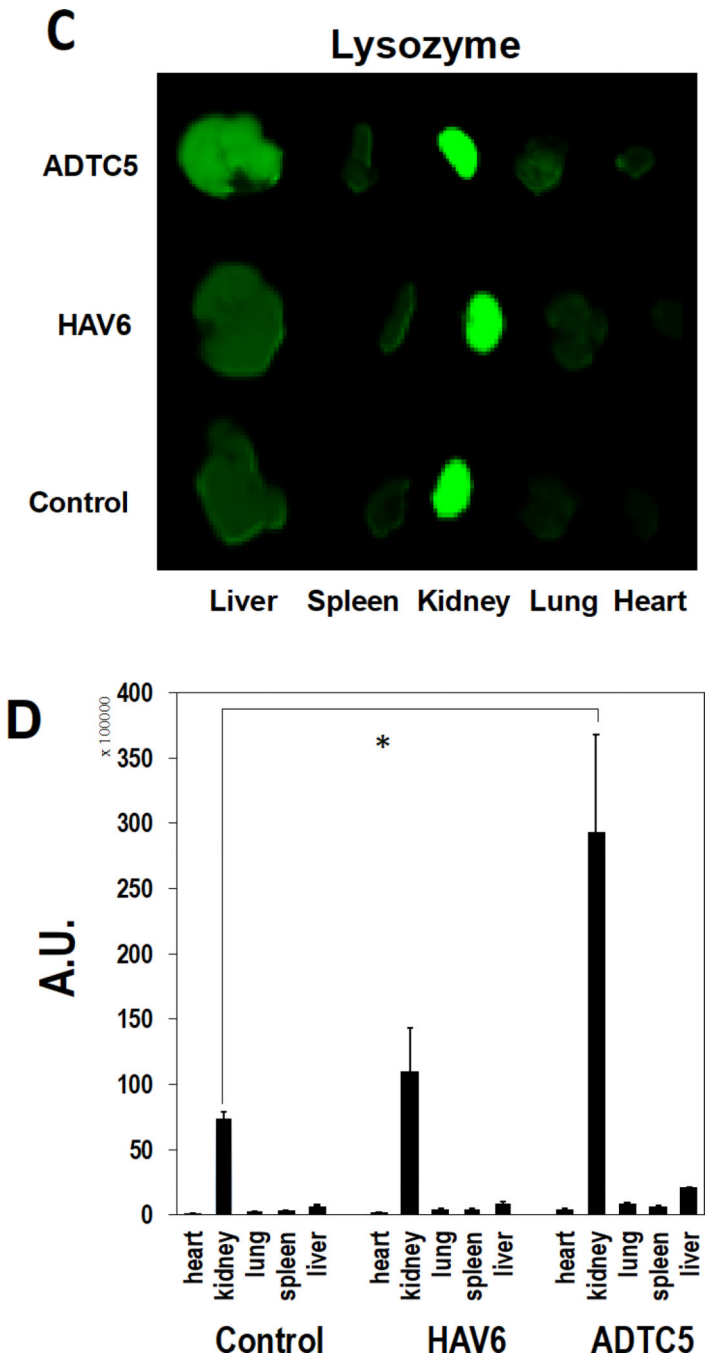

Figure 4.

Qualitative and quantitative comparisons of IRdye800CW-lysozyme (54 nmol/kg) depositions in the brain and other organs when administered alone and along with HAV6 and ADTC5 peptides (13 μmol/kg). **(A)** Qualitative comparison of NIRF brain images from control, HAV-, and ADTC5-treated animals. (B) Quantitative comparisons of lysozyme brain depositions in pmol/g brain for control, HAV6-, and ADTC5-treated mice. **(C)** Representative lysozyme depositions in heart, kidney, lung, spleen, and liver. **(D)** Comparisons of lysozyme depositions in various organs using tissue NIRF signal intensities.

A significant difference between peptide and control groups with $p < 0.05$ was designated using an asterisk (*) symbol (n = 3). The mean ± SE was used in the error bars for all groups.

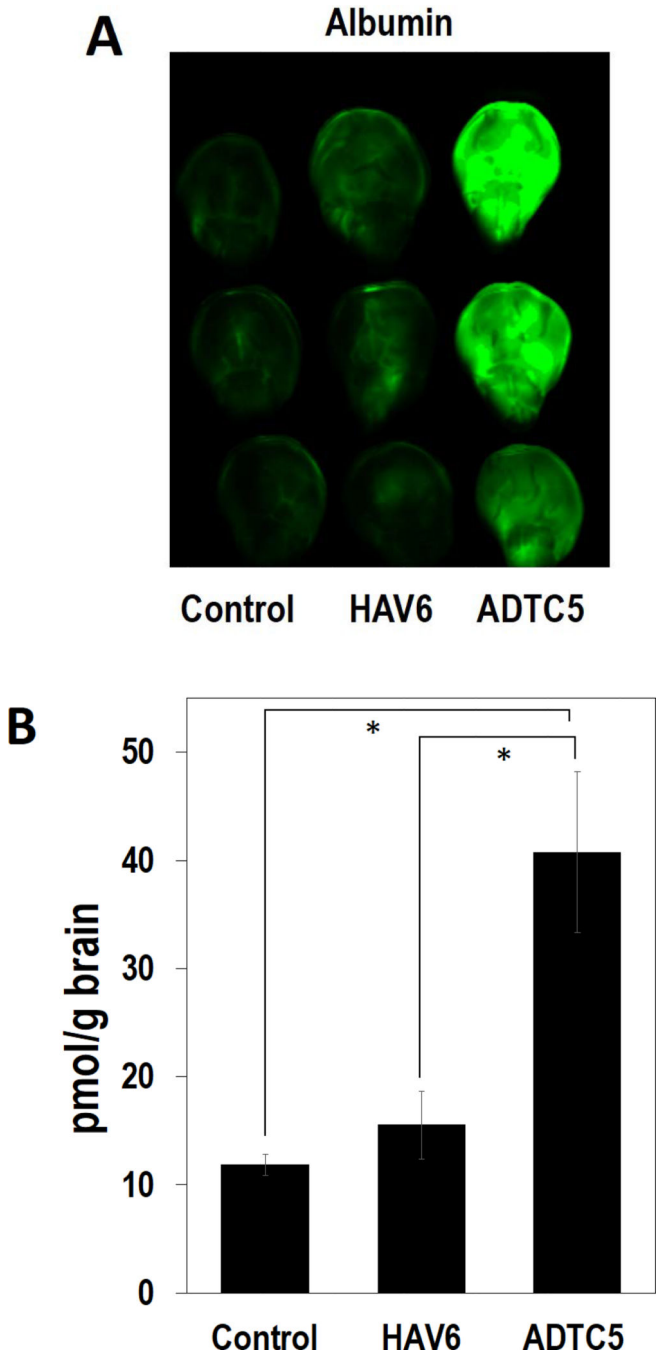

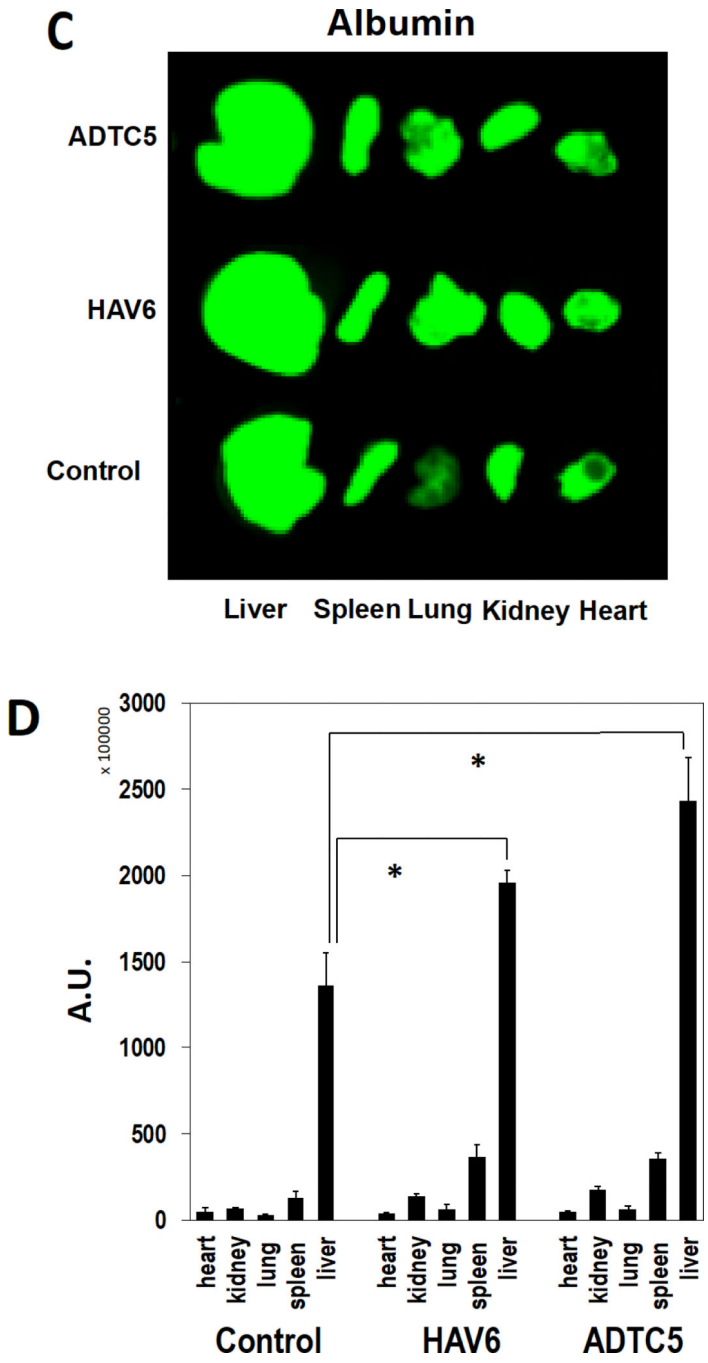

Figure 5.

Qualitative and quantitative comparisons of IRdye800CW-albumin (21.6 nmol/kg) depositions in the brain and other organs when administered alone and along with HAV6 and ADTC5 peptides (13 μmol/kg). **(A)** Qualitative comparison of NIRF brain images from control, HAV-, and ADTC5-treated animals. **(B)** Quantitative comparisons of albumin brain depositions in pmol/g brain for control, HAV6-, and ADTC5-treated mice. **(C)** Representative lysozyme depositions in heart, kidney, lung, spleen, and liver. **(D)** Comparisons of albumin depositions in various organs using tissue NIRF signal intensities.

Asterisk (*) symbol was used to indicate a significant difference with $p < 0.05$ (n = 3). Error bars were used as the mean ± SE for all groups.

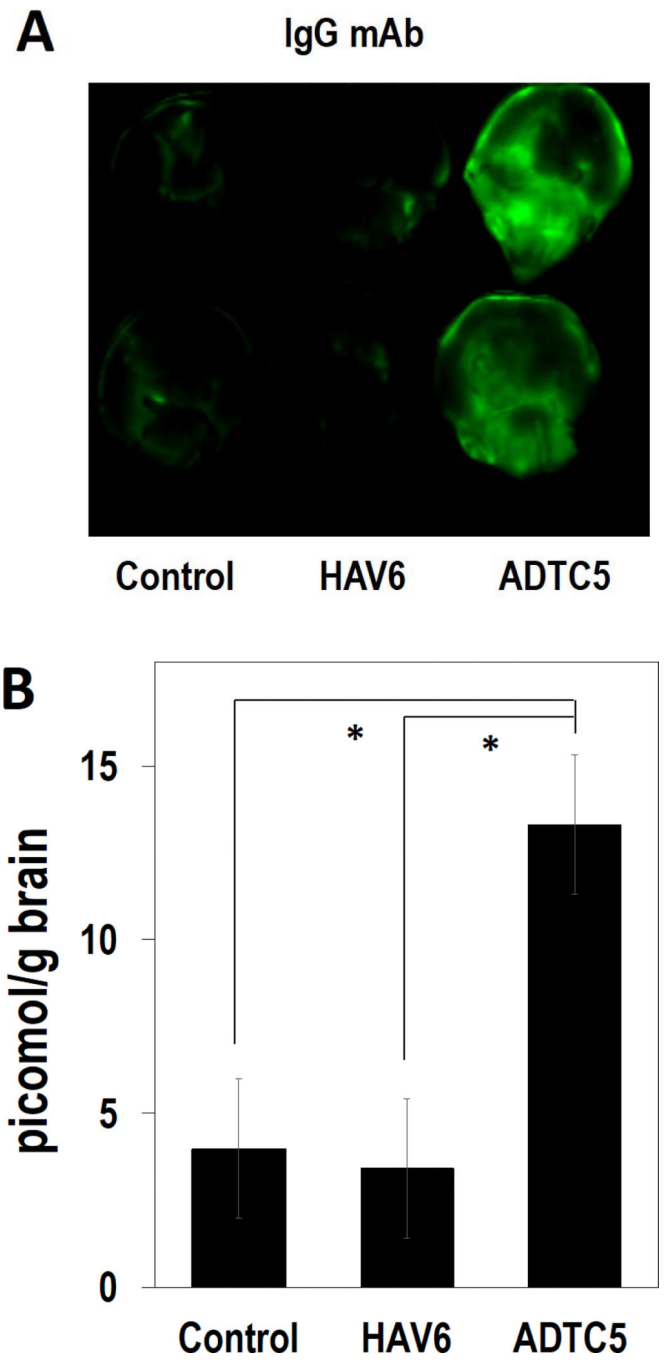

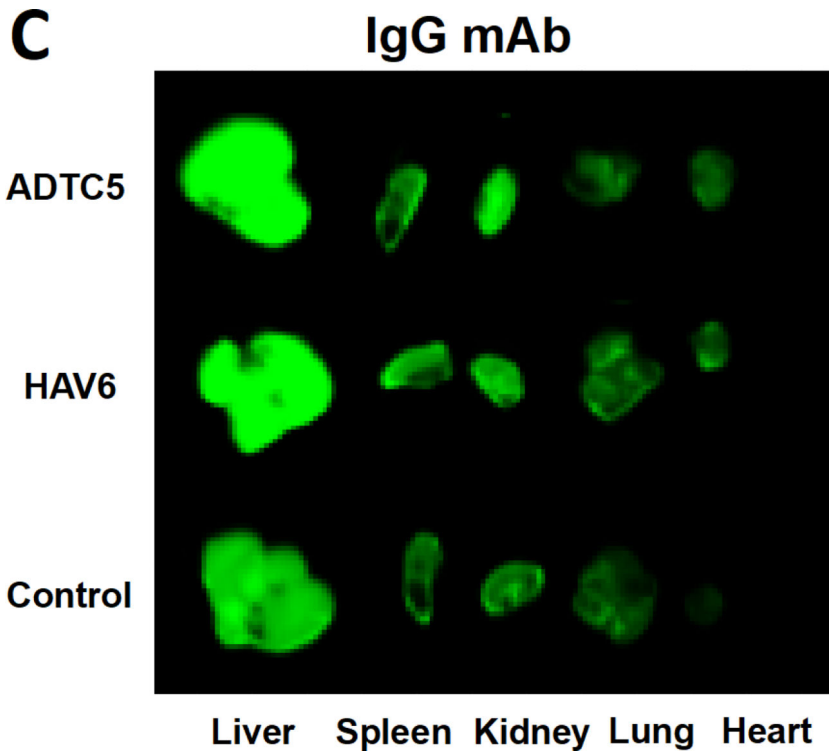

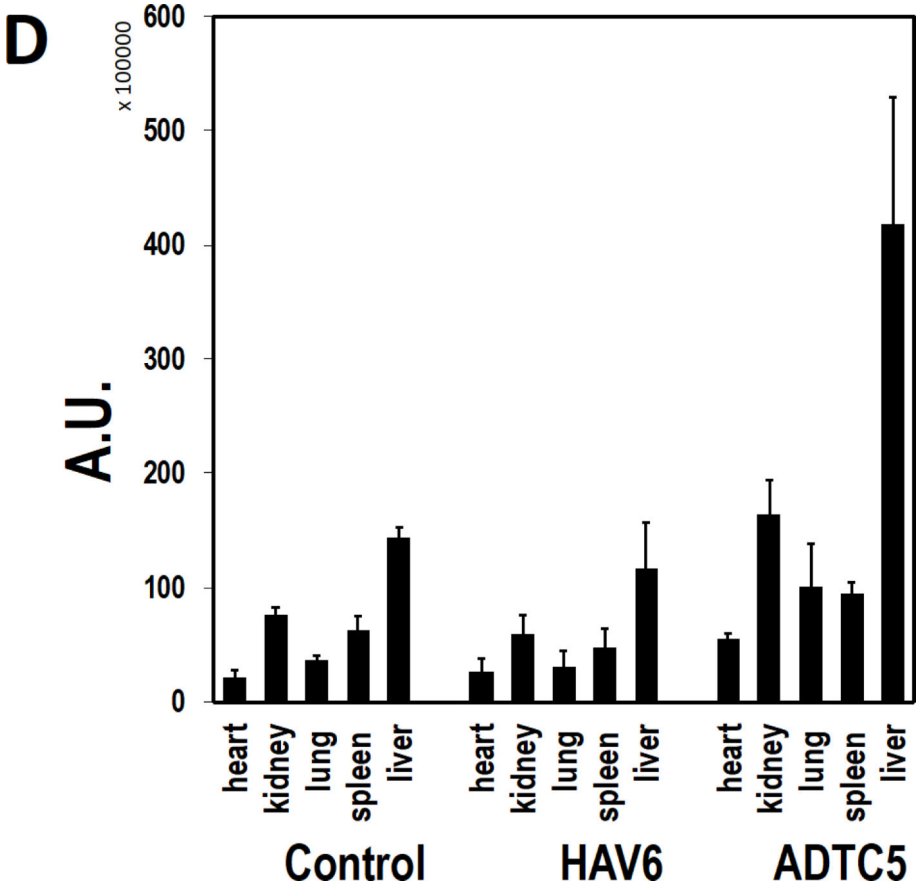

Figure 6.

Qualitative and quantitative comparisons of IRdye800CW-IgG mAb (21.6 nmol/kg) depositions in the brain and other organs when administered alone and along with HAV6 and ADTC5 peptides (13 μmol/kg). **(A)** Qualitative comparison of NIRF brain images from control, HAV-, and ADTC5-treated animals. **(B)** Quantitative comparisons of IgG mAb brain depositions in pmol/g brain for control, HAV6-, and ADTC5-treated mice. **(C)** A representative of IgG mAb depositions in heart, kidney, lung, spleen, and liver. **(D)** Comparisons of IgG mAb depositions in various organs using tissue NIRF signal intensities. A significant difference was designated using asterisk (*) with $p < 0.05$ (n = 3). The mean ± SE was used for error bars.

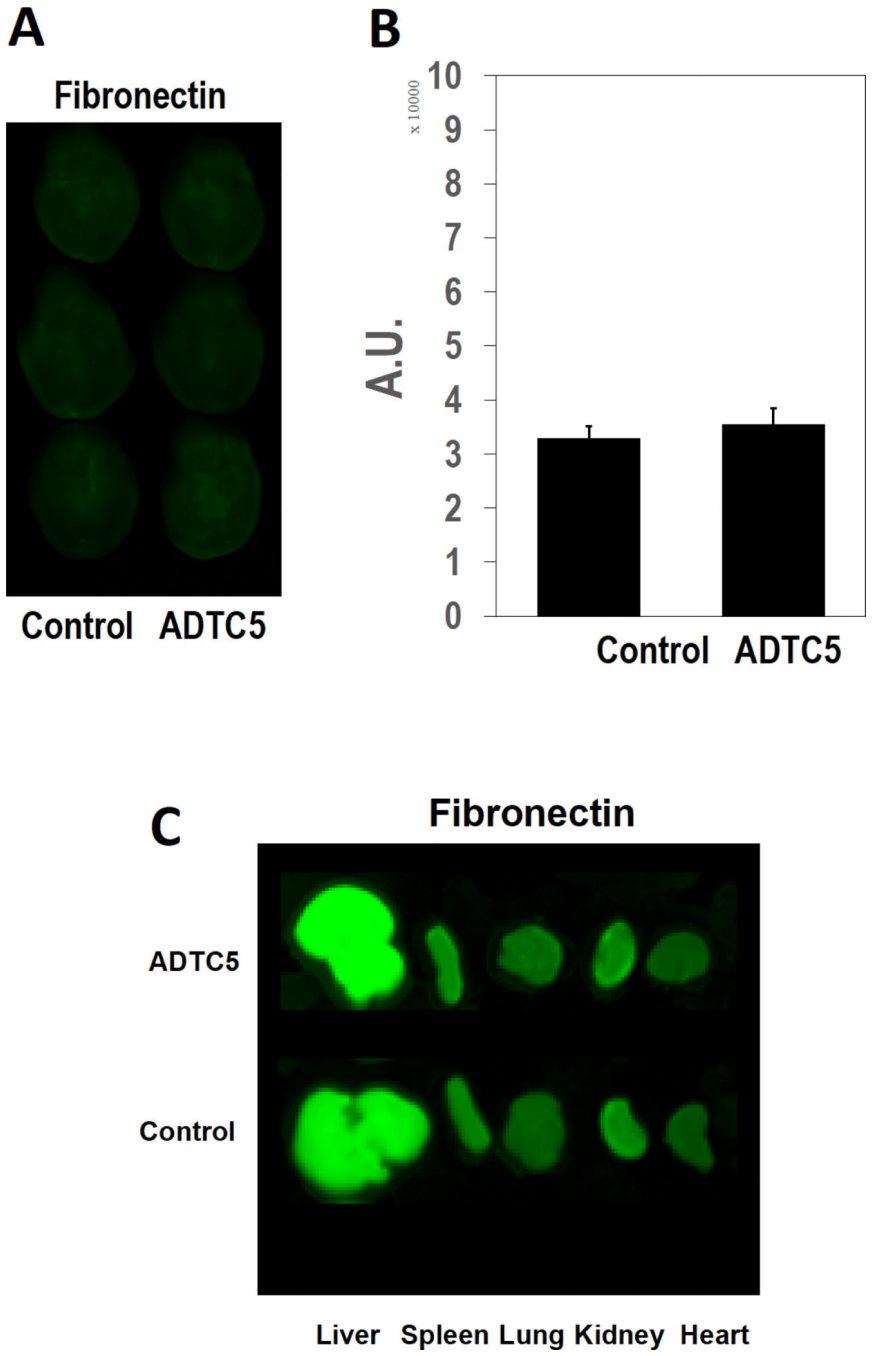

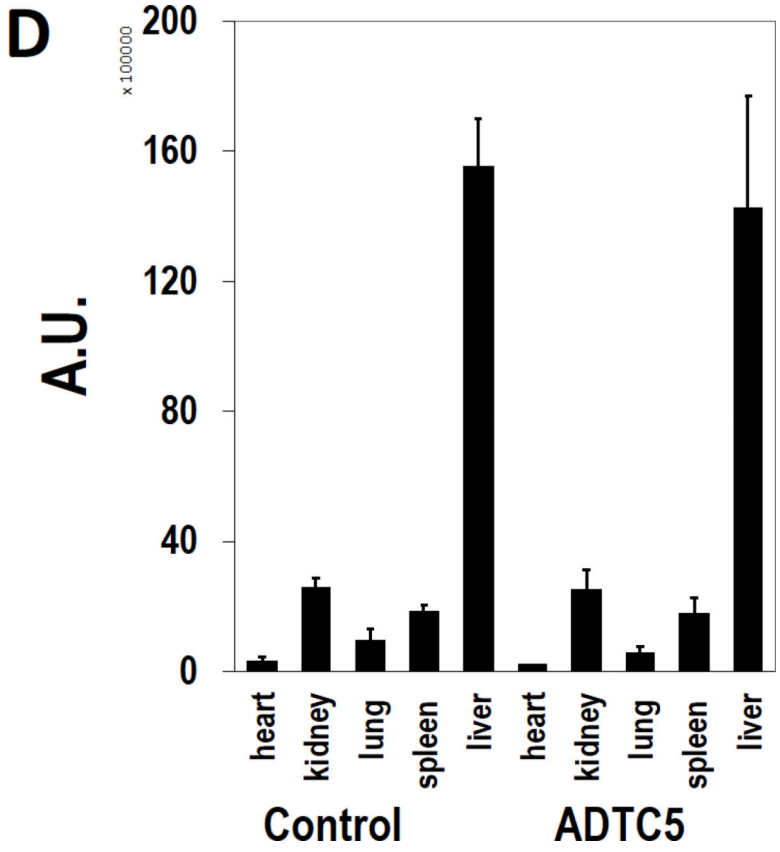

Figure 7.

Qualitative and quantitative comparisons of IRdye800CW-fibronectin (21.6 nmol/kg) depositions in the brain and other organs when administered alone and along with ADTC5 peptide (13 μmol/kg). **(A)** Qualitative comparison of NIRF brain images from control- and ADTC5-treated animals. **(B)** NIRF intensities of brain homogenates from ADTC5-treated and control mice. **(C)** A representative of fibronectin depositions in heart, kidney, lung, spleen, and liver. **(D)** Comparisons of fibronectin depositions in of various organs using tissue NIRF signal intensities. Asterisk (*) implied a statistical significance difference between two groups with $p < 0.05$ (n = 3). The mean ± SE was utilized in the error bars.

Table 1.

BBB Modulator Peptides

Peptide	Sequence	Mass (Da)	Exact Mass
ADTC5	Cyclo(1,7)Ac-CDTPPVC-NH_2	772	795.2778 (with Na^+ adduct)
HAV6	Ac-SHAVSS-NH_2	627	650.2869 (with Na^+ adduct)

Table 2.

Precision and Accuracy

Concentration (ng/mL)	Intra-day		Inter-day	
	%RSD	%RE	%RSD	%RE
0.5	15.1	7.1	10.5	6.4
5.0	4.6	−2.8	3.4	5.8
50.0	2.8	5.4	3.8	1.6

Table 3.

Stability of Protein

Concentration (ng/mL)	%RSD		
	Room Temp. (6 h)	–20 °C (24 h)	Three freeze-thaw cycles
0.5	7.7	16.2	23.1
5.0	5.4	18.5	8.5
50.0	3.7	25.1	18.4

Table 4.

Quantitative Amounts of Proteins in the Brain

Protein	Group	pmol/g brain
Lysozyme	Control	0 ± 0
	HAV6	8.3 ± 2.5
	ADTC5	37.8 ± 7.1
Albumin	Control	11.8 ± 1.0
	HAV6	15.5 ± 3.1
	ADTC5	40.7 ± 7.4
IgG mAb	Control	4.0 ± 0.4
	HAV6	3.4 ± 0.5
	ADTC5	13.3 ± 0.7